Exploiting orbital data and observation campaigns to improve space debris models

Vitali Braun
IMS Space Consultancy at Space Debris Office, ESA/ESOC, Darmstadt, Germany
André Horstmann
Institute of Space Systems, TU Braunschweig, Braunschweig, Germany
Benedikt Reihs, Stijn Lemmens, Klaus Merz, Holger Krag
Space Debris Office, ESA/ESOC, Darmstadt, Germany

ABSTRACT

The European Space Agency (ESA) has been developing the Meteoroid and Space Debris Terrestrial Environment Reference (MASTER) software as the European reference model for space debris for more than 25 years. It is an event-based simulation of all known individual debris-generating events since 1957, including breakups, solid rocket motor firings and nuclear reactor core ejections.

In 2014, the upgraded Debris Risk Assessment and Mitigation Analysis (DRAMA) tool suite was released. In the same year an ESA instruction made the standard ISO 24113:2011 on space debris mitigation requirements, adopted via the European Cooperation for Space Standardization (ECSS), applicable to all ESA missions. In order to verify the compliance of a space mission with those requirements, the DRAMA software is used to assess collision avoidance statistics, estimate the remaining orbital lifetime and evaluate the on-ground risk for controlled and uncontrolled re-entries.

In this paper, the approach to validate the MASTER and DRAMA tools is outlined. For objects larger than $1\,\mathrm{cm}$, thus potentially being observable from ground, the MASTER model has been validated through dedicated observation campaigns. Recent campaign results shall be discussed. Moreover, catalogue data from the Space Surveillance Network (SSN) has been used to correlate the larger objects.

In DRAMA, the assessment of collision avoidance statistics is based on orbit uncertainty information derived from Conjunction Data Messages (CDM) provided by the Joint Space Operations Center (JSpOC). They were collected for more than 20 ESA spacecraft in the recent years. The way this information is going to be used in a future DRAMA version is outlined and the comparison of estimated manoeuvre rates with real manoeuvres from the operations of ESA spacecraft is shown.

1 INTRODUCTION

Space debris models have been applied for many years in risk analyses and damage assessments in the early spacecraft design phases. With space debris mitigation requirements entering into force via national laws or a policy instruction making those requirements applicable for all ESA missions, the need for dedicated tools to assess the compliance with the requirements has increased correspondingly. The Meteoroid and Space debris Terrestrial Environment Reference (MASTER) model as well as the Debris Risk Assessment and Mitigation Analysis (DRAMA) tool suite have become an essential part of those compliance assessments.

In this paper, the link between the models and the observed space debris environment shall be highlighted, addressing at the same time the validation of those models.

Both, MASTER and DRAMA are going to see upgrades in the near future with new methodologies and measurement results used in that process also presented in the following, after a brief general introduction of the tools.

1.1 MASTER

The MASTER model has been developed since the 1990's as the European reference for the space debris and micrometeoroid environment. It computes flux on user-defined target orbits for object sizes down to $1\,\mu\mathrm{m}$ where each of the debris objects being part of the MASTER population originates from a dedicated source model. Each source model relies on an event database, including past launches, all known break-ups due to explosions and collisions, solid rocket motor (SRM) firings and reactor core ejection events.

Industry and academia world-wide apply the model to assess micrometeoroid and debris flux for planned satellite missions. The model output is used by different tools to perform risk and damage assessments, for instance

ESABASE2/Debris [2] or the ARES and MIDAS tools in the DRAMA software suite [10]. Moreover, MASTER is the standard model in the European Cooperation for Space Standardization (ECSS) space environment standard [4].

The latest release is MASTER-2009[1] [7] with a currently running upgrade activity to what is referred to as MASTER-8 in this paper. The data sources that are part of the MASTER population generation process are outlined in Section 2, whereas in Section 3.1 and Section 3.2 the validation process for the large and small particle population, respectively, is highlighted, showing some of the latest results from the MASTER-8 validation.

1.2 DRAMA

The DRAMA software saw its first release in 2004 with the objective to enable satellite programmes to assess their compliance with the recommendations contained in the European Code of Conduct for Space Debris Mitigation (CoC) [3, 18]. The various aspects of the mitigation guidelines have been addressed by four different tools:

1. The Assessment of Risk Event Statistics (ARES) tool allows to assess the annual rates of close approaches between an operational spacecraft and tracked objects in Earth orbits along with statistics on the required number of collision avoidance manoeuvres and associated Δv and propellant mass.

2. The MASTER-based Impact flux and Damage Assessment Software (MIDAS) facilitates the evaluation of debris and meteoroid impact rates during a satellite's lifetime and, applying single and multiple wall damage equations, the probability of penetration for a given wall design.

3. The Orbital SpaceCraft Active Removal (OSCAR) tool allows for the computation of the orbital lifetime and the evaluation of different disposal options after the End-of-Life (EOL).

4. The re-entry Survival And Risk Analysis (SARA) tool assesses which and how many components of a spacecraft would survive a re-entry and computes the on-ground casualty risk given a world population model and the impact footprint of the fragments.

With the evolution of the space debris mitigation standards in Europe, seeing the French Space Operations Act [9] come into force and the parallel development of the International Standardization Organisation (ISO) space debris mitigation standard [11], the DRAMA software was upgraded in 2014 [10]. With CROC, which allows to compute the cross-sectional areas for complex spacecraft, a new tool was added. With the ESA Space Debris Mitigation Policy, adopting the ISO 24113:2011 via the European Cooperation for Space Standardisation (ECSS) [5], coming into force in 2014, space debris mitigation requirements have become applicable to any Agency project. The DRAMA software has been identified as the main tool to support the verification of those requirements.

The different tools DRAMA offers are based on widely accepted algorithms and techniques, many of them being detailed in various specific standards. Beyond that, ARES, MIDAS and SARA make use of an extensive background knowledge on the space debris environment (for ARES and MIDAS) and analyses on the demise of spacecraft materials and the evolution of the world's population (for SARA). In this paper, the focus is on the MASTER population, as mentioned before, and a relatively new source of information that can be used to assign uncertainties to the object flux obtained from MASTER: the so-called Conjunction Data Message (CDM) and how its information content has been extracted to be used in ARES is presented in Section 2.3, whereas Section 3.3 shows the current attempts to validate the results given by ARES.

2 DATA SOURCES

The MASTER model is event-based, which means that all known space debris generating events are simulated since the beginning of the space era in 1957. Debris particles generated by a single event are propagated to so-called snapshot epochs. Each snapshot is converted to probability density tables which are then used by the flux browser in the MASTER software to re-construct a population for any given epoch in a statistical manner. While the relationship to actual objects is lost in that process, it is made sure that the overall flux characteristics are matching the ones of the underlying population. In the following sections, the MASTER event database is described.

The ARES tool uses the MASTER flux output to augment it with orbit uncertainties that are extracted from CDMs. The current approach foreseen for an upcoming DRAMA upgrade is outlined in Section 2.3.

[1] Can be downloaded from `https://sdup.esoc.esa.int`.

2.1 EVENT DATABASE

The current MASTER event database lists

- more than 5500 launches;
- more than 250 break-up events due to explosions and collisions that are currently modelled, including *assumed* events in the geostationary Earth orbit (GEO) based on the observations of object clusters in dedicated campaigns (Section 3.1);
- More than 2400 solid rocket motor firings, for which slag and dust particles are generated;
- 16 *Buk* reactor core ejection events from Soviet Radar Ocean Reconnaissance Satellites (RORSAT) in the 1980's, which resulted in the release of $5.3\,\mathrm{kg}$ of NaK droplets per event. In addition, two leakage events associated with *TOPAZ* reactors on Kosmos 1818 and Kosmos 1867, confirmed by radar measurements, are modelled in MASTER-8. [24].

All of the events are triggered in the simulation at their corresponding event epoch and associated distribution functions are then applied to obtain the size, mass, area-to-mass ratio and orbital characteristics (additional Δv) for the generated fragments. For example, the explosion and collision models are based on the National Aeronautics and Space Administration (NASA) Standard Breakup Model [12, 15][2].

Additional debris sources in MASTER are Paint Flakes and Ejecta. Both are generated in a feedback loop, where intact satellites are exposed to the simulated debris environment and surface impacts result in additional fragments (Ejecta), whereas the Extreme Ultra Violet (EUV) radiation and atomic oxygen exposure in lower orbits lead to surface degradation and the release of paint flakes. Finally, Multi-Layered Insulation (MLI) is also modelled as an individual source contribution, where MLI foils may either detach due to surface degradation processes or after a break-up of a satellite.

2.2 PUBLICLY AVAILABLE INFORMATION ON CATALOGUED OBJECTS

For objects generated via the source models described in the previous sections it may be the case that their dimensions are above the sensitivity threshold of ground-based surveillance sensors. This is especially true for break-up fragments. The Two-Line Element (TLE) catalogue contains more than $42\,000$ objects with only about $30\,\%$[3] being payloads or rocket bodies. The remaining about $70\,\%$ are either mission-related objects or debris generated in one of the events modelled in MASTER.

ESA's Database Information System Characterising Objects in Space (DISCOS) is used to augment information from the TLE catalogue by object dimensions and classification to discriminate between mission-related and other debris. This process is followed by a correlation algorithm which takes fragments generated by the break-up model and finds corresponding ones in the TLE catalogue until there are no more objects left from the set of TLE catalogue objects resulting from break-up events.

2.3 CONJUNCTION DATA MESSAGES

The risk of a collision is a crucial point to address in the design process of any satellite mission. The consequences of a collision can range from partial performance losses for a mission up to a complete fragmentation, which itself may have a considerable impact on the environment for many years, as is the case after, for instance, the Cosmos-Iridium event in 2009.

In the aftermath of the Cosmos-Iridium event, the Joint Space Operations Center (JSpOC)[4] started providing so-called Conjunction Summary Messages (CSM).

The collision avoidance (CA) support ESA's Space Debris Office (SDO) provides to ESA missions was up till then based on TLEs and additional dedicated tracking of chaser objects through TIRA upon request [1]. Since July 2010, CSMs were used, which then saw a further evolution step to the Conjunction Data Message (CDM) [22], which have been received from JSpOC and used in the CA support since March 2014.

[2] Latest statistics on debris-generating events are available from ESA's Annual Space Environment Report (`https://www.sdo.esoc.esa.int/environment_report/Environment_Report_I1R2_20170427.pdf`)

[3] `https://www.space-track.org` as of September 5, 2017.

[4] today it is referred to as the 18 Space Control Squadron (SPCS), but is used interchangeably in this paper.

A CDM comes with information on the position and velocity vectors of target and chaser satellites at the time of closest approach (TCA). Moreover, the message would usually contain the size of both objects in terms of the radar cross-section (RCS) as well as the full covariance matrix associated with the position and velocity vectors. The latter allows to estimate the collision probability, for instance via Foster's method [8], and thus to evaluate whether an avoidance manoeuvre is required or not.

Being the principal metric to define an avoidance manoeuvre threshold for a satellite mission, the collision probability needs to be assessed when it comes to model and evaluate the expected manoeuvre rate in the design process of a mission. To achieve this, the ARES tool would take the impact flux obtained from MASTER and assign uncertainties to them prior to computing the collision probability. In the first DRAMA version in 2004, uncertainties originated from a dedicated TLE analysis. It was decided to apply them for a defined set of orbit classes observing that uncertainty in an object state is affected by

- the perigee altitude, where lower altitudes mean higher drag perturbations but also more difficulties in obtaining ground-based observations in the perigee region;
- the inclination where, again, a lower inclination may result in worse observability due to the sensors being distributed preferably at higher latitudes;
- the eccentricity which, in combination with the perigee altitude, again may impose observability constraints and thus result in lower quality information for an orbit.

In addition to that, the subdivision into orbit classes also depends on the available data to cover those classes. For DRAMA 1, based on TLE information only, there were three perigee altitude classes ($0 < h_p \leq 800$; $800 < h_p \leq 25\,000$ and $h_p > 25\,000$), three inclination classes ($0° \leq i < 30°$; $30° \leq i < 60°$ and $60° \leq i \leq 90°$) and two eccentricity classes ($e \leq 0.1$ and $e > 0.1$).

In DRAMA 2, the number of classes was extended to provide a better resolution, given the new set of information coming from the CSMs. Additional size classes were introduced based on RCS, as smaller objects tend to have poorer orbit information than larger ones. In total, about 200 CSMs were used. Given the number of orbit classes, there were still many gaps. Especially for the high eccentricity cases, with essentially no spacecraft operated in those orbits and also no chaser objects from high eccentric orbits that could have been part of conjunction events CSMs were received for. Hence, TLEs were still required to fill the gaps and techniques were developed to map TLE uncertainties to CSM ones by analogies: for example, for those classes, where both TLE and CSM information was available, it was possible to obtain a mapping factor between them and apply that factor to classes where there were only TLEs but no CSMs.

The situation changed drastically with the advent of the CDM. Since March 2014, SDO has received about 1 million CDMs. With one CDM providing information about two objects, the total data set was about 2 million. Based on this new information, also the class definitions have been revised and the current classification is given in Table 1. The

Tab. 1: New class definition for the ARES CDM uncertainty lookup tables.

Index	Size (RCS) s / m^2	Eccentricity e / -	Perigee altitude h_p / km	Inclination i / deg
1	$s < 0.1$	$e < 0.1$	$h_p \leq 350$	$0 \leq i < 15$
2	$0.1 \leq s \leq 1.0$	$e \geq 0.1$	$350 < h_p \leq 550$	$15 \leq i < 30$
3	$s > 1.0$		$550 < h_p \leq 800$	$30 \leq i < 45$
4			$800 < h_p \leq 2000$	$45 \leq i < 60$
5			$2000 < h_p \leq 25\,000$	$60 \leq i < 75$
6			$h_p > 25\,000$	$75 \leq i \leq 90$

number of data points for each class, specified by a combination of indices for the size, eccentricity, perigee altitude and inclination, is shown in Figure 1. The three size classes are now in line with the definition of *Large*, *Small* and *Medium* sized objects as published regularly in the Satellite Situation Report (SSR)[5] for objects in the TLE catalogue. Note that the numbers given in Figure 1 are logarithmic. For instance, there are about $10^{5.8} \approx 600\,000$ CDMs contributing to the class (s_3, e_1, h_{p3}, i_6) in Figure 1a. The notation (s_i, e_j, h_{pk}, i_l) refers to the size, eccentricity, perigee altitude and inclination class with indices i, j, k and l, respectively, according to Table 1.

[5] `https://www.space-track.org`

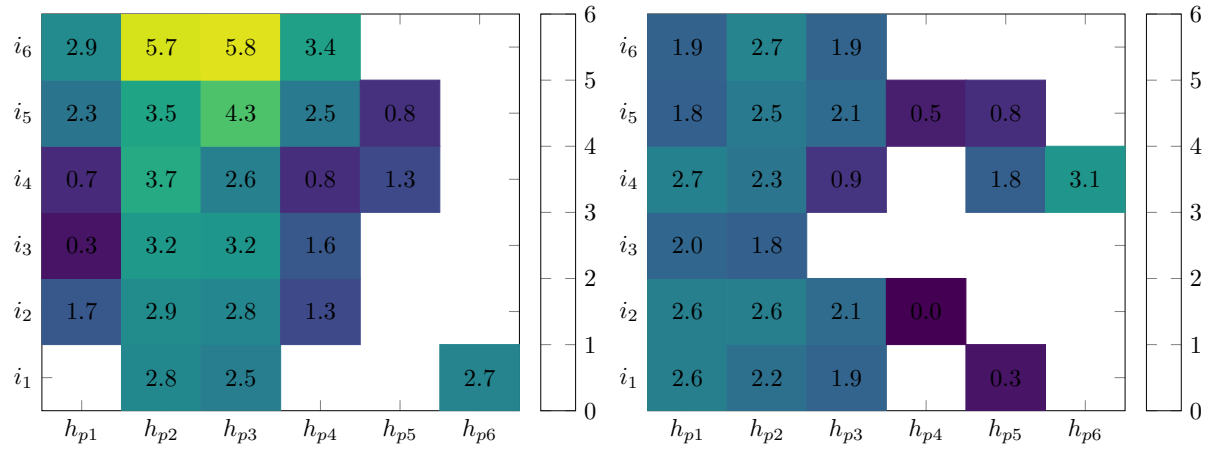

(a) Large objects, e < 0.1.

(b) Large objects, e ≥ 0.1.

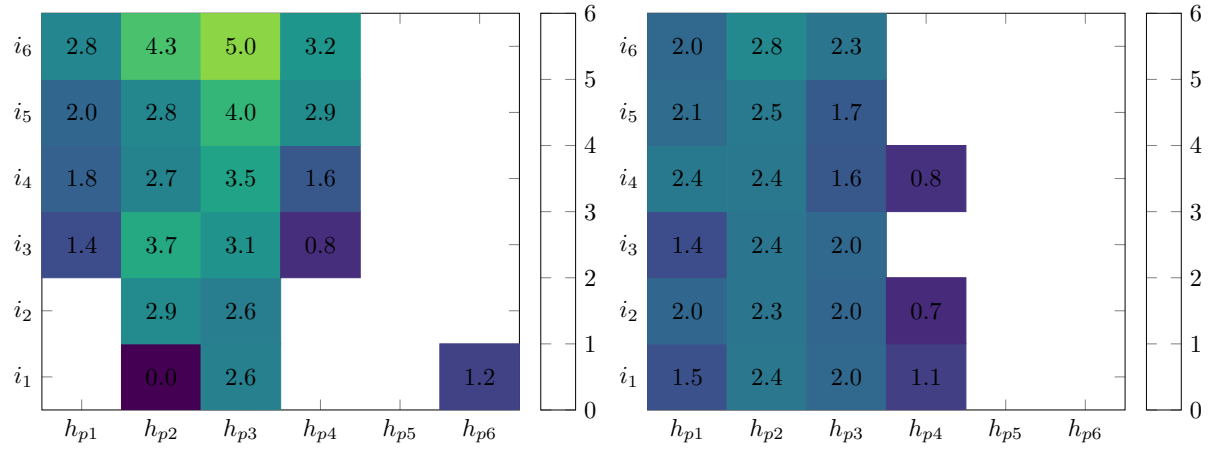

(c) Medium objects, e < 0.1.

(d) Medium objects, e ≥ 0.1.

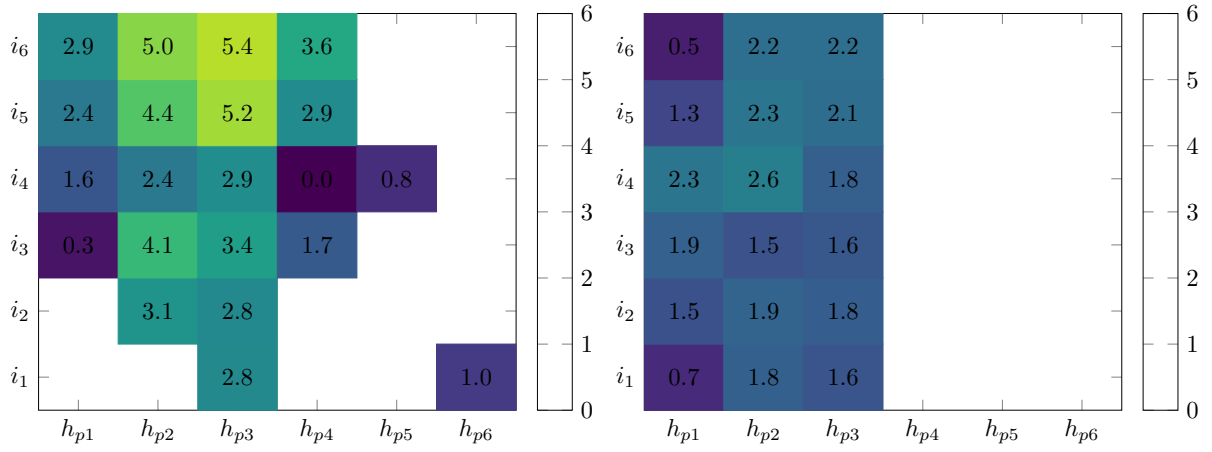

(e) Small objects, e < 0.1.

(f) Small objects, e ≥ 0.1.

Fig. 1: ARES class definition and data coverage solely based on CDMs. Number N of CDMs displayed as $lg(N)$. Classes without data without color and number.

Even though there are still gaps, where there were no CDMs to provide information for specific classes, the situation clearly improved compared to DRAMA 2. Examples are the high altitude orbits (h_{p4}, h_{p5}, h_{p6}), where ESA missions like LISA Pathfinder, Sentinel 3A and Galileo contributed. Moreover, it has been possible to cover high-eccentricity orbits ($e \geq 0.1$) now directly (as opposed to the TLE-based approach in DRAMA 2), for example via ESA's Cluster-II satellites (seen especially with about 1000 CDMs in (s_3, e_2, h_{p6}, i_4) in 1b).

For each of the classes, three functions were defined to obtain the uncertainties $(1-\sigma)$ in the radial (U), along-track (V) and normal (W) directions in the satellite-centered reference frame[6]:

$$\sigma_j = c_j \cdot 10^{a_j \cdot \Delta t},\ j \in (U, W) \tag{1}$$

$$\sigma_V = c_V \cdot (b_V + \Delta t)^{a_V} \tag{2}$$

The coefficients c_j, a_j, c_V, a_V and b_V of those equations are estimated in a linear regression process for each class from the CDM data as a function of the time interval Δt between the TCA and the CDM creation date. This allows to define in ARES the time interval between the close approach event and the time a potential collision avoidance manoeuvre would be implemented in real operations. The general tendency is that uncertainties get smaller for decreasing Δt.

Being a rather straightforward approach for those classes where a lot of data points are available, the more difficult part is to take care of those classes where only sparse data or even no CDMs are available. The regression can only be considered *valid* from a statistical point of view, if there are enough data points - for several reasons:

- It fails technically, if there are fewer CDMs than the mathematical model requires, e.g. only one CDM as for (s_2, e_1, h_{p2}, i_1) or (s_1, e_2, h_{p4}, i_2);
- For only a few CDMs, the corresponding size class could be dominated by a single or only a few events which could result in a significant systematic error;
- Repeating conjunction events, where the target satellite would see the same chaser once every revolution for a given time period on the order of days, in combination with potentially poor information on the chaser's orbit and thus lacking updates over time, might result in an additional bias for the estimated coefficients.

Based on a visual inspection of the distributions for each class, it was therefore decided to set the minimum number of CDMs to $N = 100$ (or $lg(N) = 2.0$) for a class to be considered valid. There are, however, some classes, where the result appeared to be acceptable (without any of the features described above) event with $N < 100$, for instance (s_1, e_1, h_{p4}, i_3) (48 CDMs) or (s_2, e_1, h_{p1}, i_5) (95 CDMs).

For the remaining classes with too few CDMs or even no data, a similar technique as in the previous DRAMA version has been applied (see also Figure 1 for reference):

1. For a given set of classes (s_i, e_j, h_{pk}, i_l) with i, j, k constant and $l \in (1, 6)$, if there is at least one l the associated class is considered valid for:
   - Copy directly from the neighbour class, e.g. by taking the coefficients obtained from (s_1, e_1, h_{p1}, i_4) and apply them also to $(s_1, e_1, h_{p1}, i_l),\ l \in (1, 3)$; or
   - Perform a regression over all non-empty inclination classes combined, e.g. by taking $(s_3, e_1, h_{p1}, i_l),\ l \in (5, 6)$ and apply the result to $(s_3, e_1, h_{p1}, i_k),\ k \in (1, 4)$.
2. If there is not a single valid class for (s_i, e_j, h_{pk}, i_l) with i, j, k constant and $l \in (1, 6)$, for instance for (s_2, e_1, h_{p5}, i_l), a combination of the inclination and size classes is performed. Hence, the class (s_2, e_1, h_{p5}, i_l) in this example would be filled by a combined solution with CDMs from $(s_i, e_1, h_{p5}, i_l),\ i \in (1, 3),\ l \in (1, 6)$.

There is a strong argument in saying that low inclination classes in LEO would tend to have higher uncertainties due to observability constraints and thus the approach via Rule 1 would under-estimate those uncertainties by copying them from higher inclination classes. Several subsets of classes have been analysed with the result that the above argument is true in some cases, but not in general. It is possible that this observation could be credited to a too small data set, but there is no definite answer at the moment. Hence, it was decided to keep with the above set of rules until additional data collected in the future would allow for a more prudent study of these effects.

[6]The same reference frame the covariance matrix is provided for in the CDM.

3 VALIDATION OF SPACE DEBRIS MODELS

Any space debris model requires a validation process based on the observation of the environment in order to see if the model predictions match what has been observed. For the space debris environment, the challenge is to obtain the required measurements for a full validation. While ground-based observation campaigns are used to sample the large object population (Section 3.1), one has to rely on returned surfaces and impact detectors for the small object population (Section 3.2). Manoeuvre rates predicted by ARES can be verified by looking at the real number of performed collision avoidance manoeuvres (Section 3.3).

3.1 LARGE OBJECT POPULATION

Dedicated ground-based observation campaigns have been performed since the beginning of the development of space debris models. Currently, the subset of the MASTER population that is detectable from ground is validated using contributions from

- the publicly available TLE catalogue, where objects of the MASTER population are correlated with objects from TLE as outlined in Section 2.2. As a rule of thumb, the sensitivity limit for the US Space Surveillance Network (SSN) to keep objects in the catalogue is typically reported as $10\,\mathrm{cm}$ for the LEO and $1\,\mathrm{m}$ for the GEO region (e.g. [13]);
- the ESA Space Debris Telescope (SDT) on the island of Tenerife, Spain (Figure 2c). The $1\,\mathrm{m}$ Ritchey-Chrétien telescope, with a Field of View (FOV) of $0.7°$ has been used since 2001 in yearly survey campaigns accumulating more than 800 nights (about $6000\,\mathrm{h}$) of observation time mainly for the GEO region but also for satellites in the Medium Earth Orbit (MEO) region. Already the first campaign in 2001 revealed a large number of uncorrelated (wrt. the TLE catalogue) objects in the range from magnitude 15 to 21 [19]. Moreover, later campaigns contributed the knowledge of the sub-population of so-called High-Area-to-Mass-Ratio (HAMR) objects, which resulted in a new debris source model that was added to MASTER in its 2009 version;
- the Tracking and Imaging Radar (TIRA) in Wachtberg, Germany (Figure 2a). A $34\,\mathrm{m}$ parabolic dish antenna is operated in a monopulse tracking mode in the L-band ($1.333\,\mathrm{GHz}$, $1\,\mathrm{MW}$ peak power) and Ku-band ($1.67\,\mathrm{GHz}$, $13\,\mathrm{kW}$ peak power) for Synthetic Aperture Radar (SAR) imaging. Data from beam-park experiments (BPE) surveying the LEO region since 2000 is used, accumulating about $260\,\mathrm{h}$ of observations. The detection threshold at $1000\,\mathrm{km}$ is at about $2\,\mathrm{cm}$, whereas bi-static campaigns with the Effelsberg $100\,\mathrm{m}$ radio telescope allowed to decrease the sensitivity limit to $0.9\,\mathrm{mm}$ [13]. While most of the campaigns were East-staring, TIRA was used in a South-staring mode (S-BPE) in 2015 to obtain detections for lower inclination orbits;
- the European Incoherent Scatter (EISCAT) network of ionospheric research radars in Finland, Norway and Sweden (Figure 2b). Space debris measurements have been obtained simultaneously with the ionospheric measurements by the EISCAT radars and were used for the first time in the validation of MASTER-2009 with more than 100 days of observation time ($24\,\mathrm{h}$ each) from 2007 to 2009. Objects down to $2\,\mathrm{cm}$ size are detectable at a range of $1000\,\mathrm{km}$ [17].

Besides the sensors mentioned above, $345\,\mathrm{h}$ of Haystack observations (X-band) from the 1990's were used [14]. Moreover, the Haystack radar contributed significantly to the characterisation of the NaK droplet population in altitudes around $900\,\mathrm{km}$ due to their special reflection properties [16]. The NaK model used in MASTER saw several evolution steps since its first implementation in the 1999 version and today shows an excellent fit to the measured size distribution [25].

Figure 3 shows a comparison of the size distribution for the most recent campaigns by TIRA (Figure 3a) and EISCAT (Figure 3b)[7].

The MASTER population is filtered by the Program for Radar and Optical Observations Forecasting (PROOF) in order to come up with actual detection statistics for the specific sensor. The size distributions for both campaigns show a decent match with the simulated detection rates of the MASTER population. However, there are few important subtleties in such a comparison. First of all, radars do not measure the object size directly. With an obtained range measurement and the corresponding Signal-to-Noise (SNR) ratio, one can compute the Radar Cross-Section (RCS). The relationship to the actual size of the object depends on the wavelength, conductive properties, etc. There may be

[7] With the validation of the MASTER population on-going, all presented results are considered preliminary in this paper

(a) The Tracking and Imaging Radar (TIRA) in Wachtberg, Germany. Credits: FHR Fraunhofer

(b) The European Incoherent Scatter Scientific Association (EISCAT) Svalbard radar facility near Longyearbyen. Credits: EISCAT

(c) The 1 m Optical Ground Station (OGS) telescope in the Teide Observatory. Credits: ESA

Fig. 2: Sensors contributing to the MASTER large object population validation.

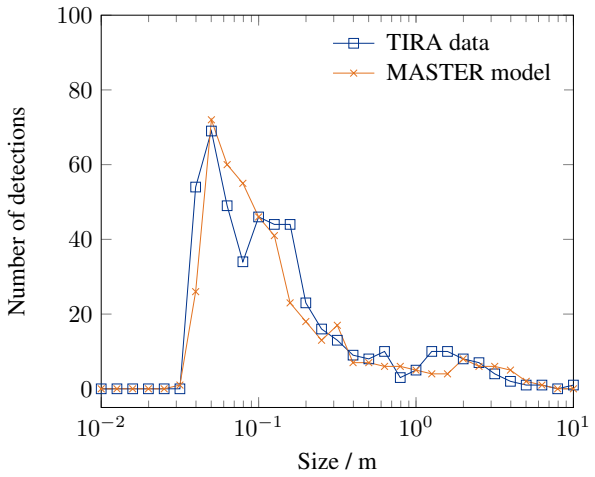

(a) TIRA S-BPE, Dec 8, 2015.

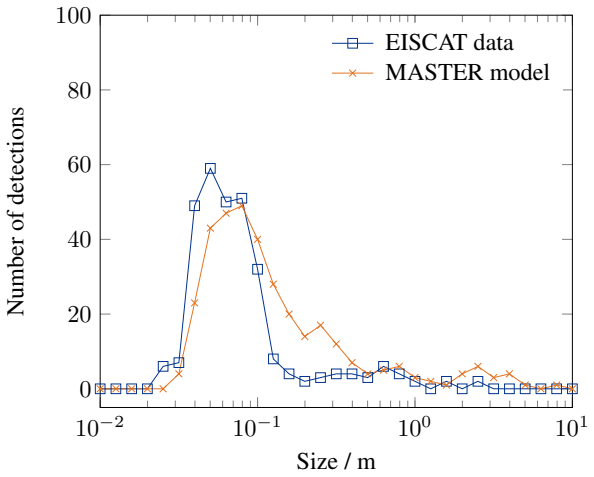

(b) EISCAT, Oct 23, 2015.

Fig. 3: Comparison of simulated observations based on the MASTER population with recent measurement campaigns by TIRA and EISCAT for the LEO region. **Note:** The results are preliminary, as the current validation of the MASTER upgrade is on-going.

ambiguities resolving the size in the Mie region, where the objects' characteristic length is similar to the wavelength of the radar signal.

Moreover, while the TIRA radar allows to determine where within the radar beam an object was detected, this is not possible with EISCAT. Effectively, this leads to a minimum RCS that is obtained and therefore a potentially biased size distribution towards smaller sizes [17].

For the GEO region, a comparison to the SDT measurements in 2007 is shown in Figure 4a. There have been a few confirmed fragmentations in GEO, like the Titan 3C Transtage (1968-081E) event from 1992 (shown in Figure 4b), which appear as point clusters in the Inclination vs. Right Ascension of Ascending Node (RAAN) plot. As MASTER is purely event-based, a few additional break-up events have been modelled [6] in order to match such observed clusters and thus to provide a more accurate estimate of the flux in the GEO region. The list of unconfirmed events is being revised with any new measurements.

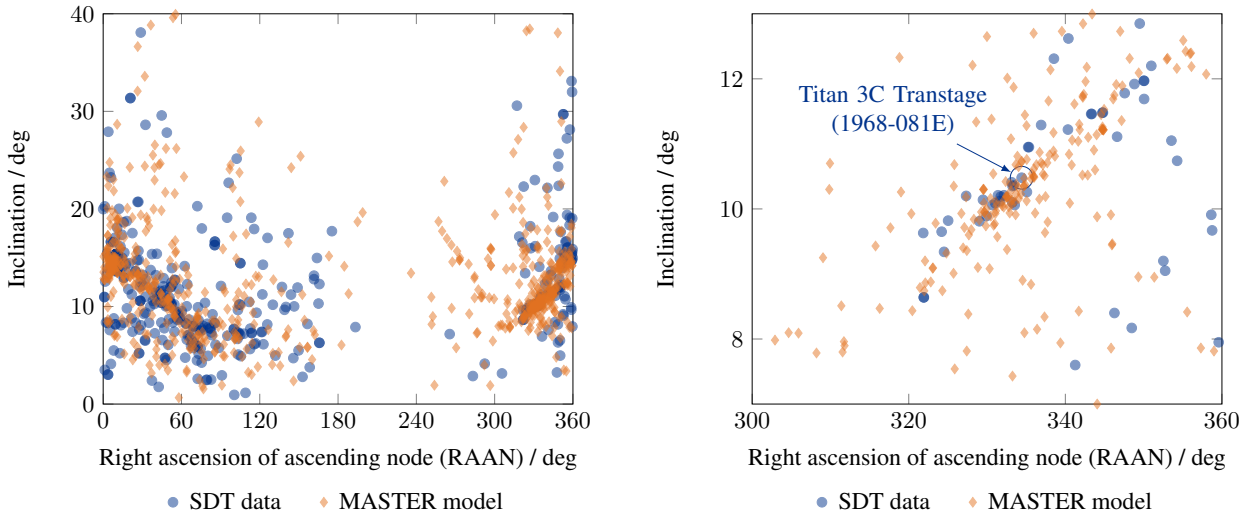

(a) SDT, Jan 2007.

(b) Zoom-in on region around 1968-081E fragments.

Fig. 4: Comparison of simulated observations based on the MASTER population with the SDT GEO campaign in 2007. **Note:** The results are preliminary, as the current validation of the MASTER upgrade is on-going.

3.2 SMALL OBJECT POPULATION

The validation of the small object population is currently based on the analysis of impact features on surfaces returned from space. It is foreseen to extend the database and include also data from in-situ measurements. Usually, the latter would have significantly reduced detection cross-sections compared to the returned surfaces and thus lower impact counts. However, it would still make sense to include them in order to obtain more data points in space and time.

The following returned surfaces are part of the current validation process:

- The Long Duration Exposure Facility (LDEF, Figure 5b) was launched in April 1984 by the Space Shuttle mission STS-41-C into an altitude of about $480\,\mathrm{km}$. The nominal mission duration of about one year saw a delay with LDEF finally recovered by STS-32 in January 1990. This was a fortunate coincidence for the space debris community (but also others) as it had been sampling the environment for more than 2000 days.
- The European Retrievable Carrier (EuReCa, Figure 5c) was an ESA mission launched by STS-46 in July 1992 into an altitude of about $440\,\mathrm{km}$ and manoeuvred itself into an orbit of $508\,\mathrm{km}$ altitude. It carried multiple experiments and was intended to be launched multiple times. However, after its retrieval by STS-57 in July 1993, subsequent flights were cancelled.
- Replaced solar arrays from the Hubble Space Telescope (HST, Figure 6a) Service Missions SM-1 and SM-3B, conducted during the Space Shuttle flights STS-61 in December 1993 and STS-109 in March 2002, respectively. Three solar arrays were returned to ESA with two of them after an exposure to the space environment at about $600\,\mathrm{km}$ for more than seven years.

Figure 6 shows exemplary results for the HST-SM1 (Figure 6a) and the EuReCa (Figure 5c) solar arrays.

Impact counts were obtained for the retrieved surfaces as a function of the conchoidal diameter. In order to compare them to flux levels from the MASTER population, the latter have to be processed via well-known damage equations for solar arrays. Both figures show a good match, which is especially true for conchoidal diameters between $0.03\,\mathrm{mm}$ to $1\,\mathrm{mm}$ for HST-SM1 and $0.02\,\mathrm{mm}$ to $1\,\mathrm{mm}$ for EuReCa, respectively. As damage assessments for satellite missions are usually performed for impactor sizes in that regime, a good representation of the actual flux is highly desirable.

Similar results as those shown in Figure 6 are also obtained for the different analysed surfaces of LDEF. An additional remarkable result was the explanation of distinct impact signatures known in literature as *May Swarms* that were observed on surfaces of the Interplanetary Dust Experiment (IDE) carried by LDEF. Figure 7 shows the measured impact right ascension vs. time after deployment of LDEF (in red). From the database of SRM firings, it was possible to correlate the May Swarms with two firing events of the ill-fated Westar 6 and Palapa B2 satellites (both were

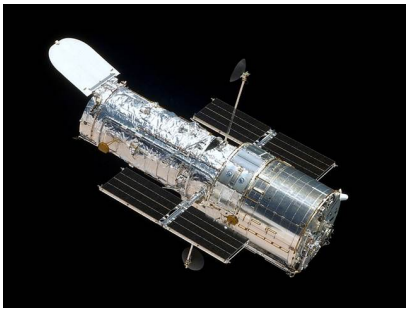

(a) The Hubble Space Telescope. Credits: NASA

(b) The Long Duration Exposure Facility (LDEF). Credits: NASA

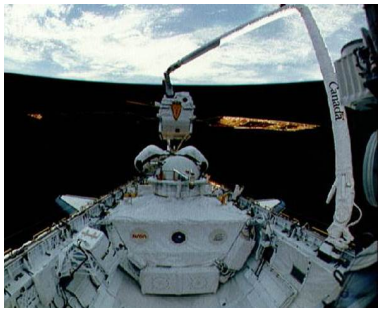

(c) The European Retrievable Carrier (EuReCa). Credits: NASA

Fig. 5: Retrieved surfaces of the shown satellites allow for the MASTER small object population validation.

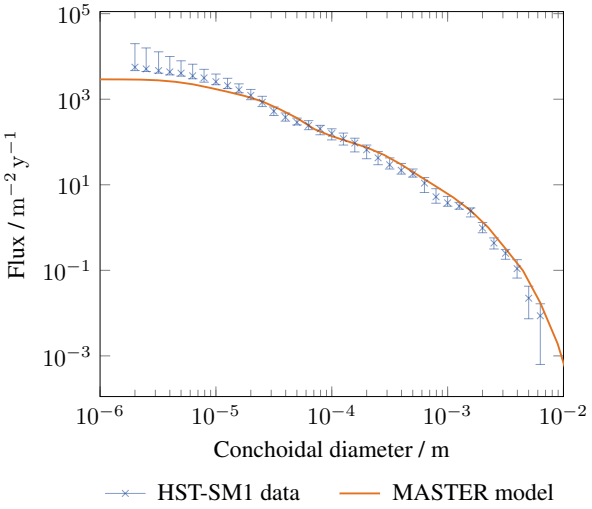

(a) HST-SM1 solar array front.

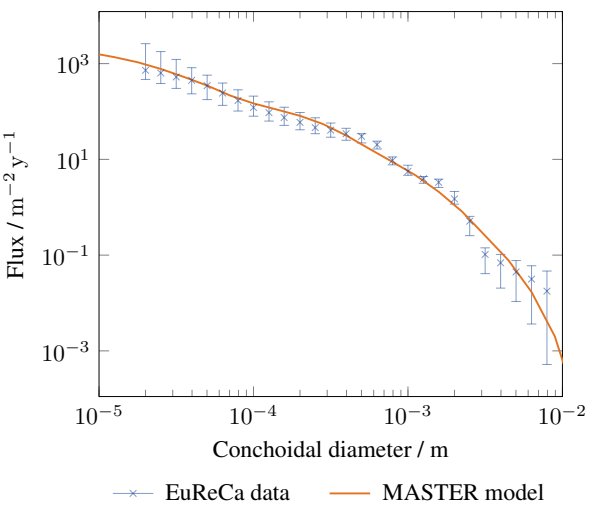

(b) EuReCa solar array front.

Fig. 6: Comparison of simulated impacts based on the MASTER population with retrieved surfaces from the Hubble Space Telescope (HST) and the European Retrievable Carrier (EuReCa). **Note:** The results are preliminary, as the current validation of the MASTER upgrade is on-going.

recovered during STS-51A later that year) [20]. Moreover, later analyses of Soviet photo-reconnaissance satellites' retro-firings revealed allowed to correlate additional cluster features with actual firing events [23]. For example, the Kosmos satellites also shown in Figure 7 were all of the Zenit type which allowed for the recovery of the satellite's telescope after a re-entry of the payload module.

3.3 COLLISION AVOIDANCE MANOEUVRE RATES

The model to predict collision avoidance manoeuvre rates has been outlined in Section 2.3. However, at the time of writing for this paper, the validation including the new data from the CDMs has not yet finished. Therefore, the validation of the previous ARES version (ARES v2.18.2, based on CSM and TLE data) is outlined.

The SDO provides a collision avoidance service as an operational support to many ESA missions but also third party customers. In Table 2, the number of actually performed collision avoidance manoeuvres of selected ESA missions are shown since 2009, compared to the ARES predictions. It should be noted that although some of the average manoeuvre rates match quite well with the model, there are currently no direct conclusions that could be drawn from this analysis, due to several aspects:

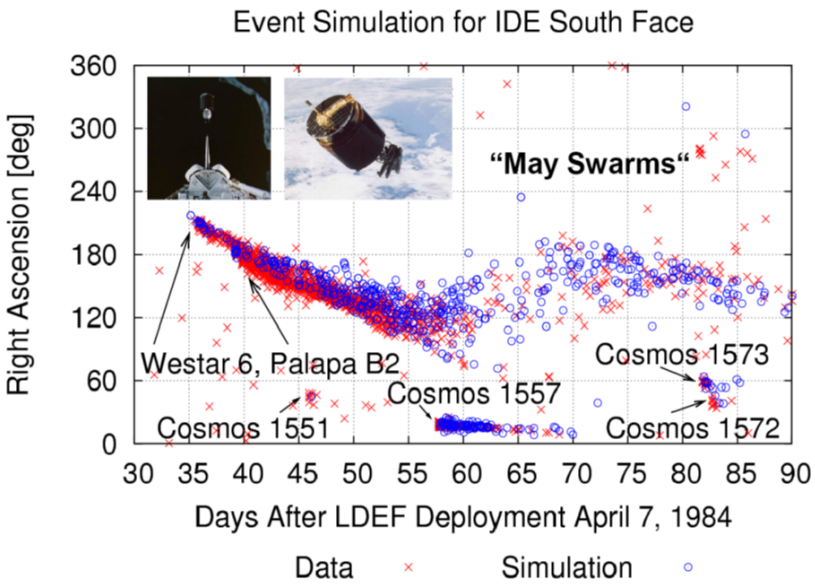

Fig. 7: Identification of impact signatures on the LDEF IDE South Face via the MASTER model [20, 21, 23].

- In general, collision avoidance manoeuvres happen rather rarely, so the data given in Table 2 at the moment leads to low-number statistics. This is especially true, for instance, in the case of the Swarm satellites.
- The ARES version 2.18.2 is based on CSM and TLE data, whereas the collision avoidance service since March 2014 is based on CDMs only. Especially for a TLE-based approach, the false alarm rate - which in itself is arduous to assess - is considered to be higher compared to CDMs.
- Former collision avoidance procedures, principally for Envisat and ERS-2, included the option to obtain additional tracking of the chaser object (via TIRA). This is not modelled and essentially would mean a too high number of expected manoeuvres.
- Many of the satellites in Table 2 perform nominal orbit control manoeuvres (OCM). Some of the events counted into the statistics in Table 2 are actually modified OCMs that minimised a post-manoeuvre close approach risk of a foreseen event. Without an OCM, it could also happen that there would not be an avoidance manoeuvre after a potential orbit update prior to the event.

Tab. 2: Latest statistics on collision avoidance manoeuvres for ESA missions supported by the Space Debris Office. Comparison with manoeuvre rates obtained with the current ARES version.

Mission	Year								Average	ARES v2.18.2
	2009	2010	2011	2012	2013	2014	2015	2016	# / y	# / y
Envisat	2	4	4						3.3	2.8
ERS-2	0	4	1						1.7	1.9
Sentinel 1A						8	4	4	5.3	2.9
Sentinel 1B								3	3.0	2.9
Sentinel 2A							0	2	1.0	2.3
Sentinel 3A								1	1.0	1.2
Cryosat 2		1	0	1	2	3	4	1	1.7	0.4
Swarm A						1	0	0	0.3	1.0
Swarm B						0	1	1	0.7	1.2
Swarm C						0	0	0	0.0	1.0

- There were single events which had a collision probability above the manoeuvre threshold, but it was too late to implement it as the notification came in on short notice. All ARES simulations were based on $\Delta t = 24h$. It happened also in several instances that actually planned avoidance manoeuvres (and, potentially, already uplinked to the satellite) were cancelled after a late update on the event with $\Delta t < 24h$.

4 CONCLUSION

The methodology to derive state uncertainties to be associated with object flux in DRAMA/ARES based on CDM data has been outlined in this paper. It is the first time uncertainties for all defined orbit and size classes are derived solely from CDM statistics. The implementation into the DRAMA software is currently on-going. ESA satellites are continuing to collect CDMs and are likely to conduct additional manoeuvres in the near future. Therefore, it is expected that future analyses similar to the one shown in Table 2 can be conducted based on higher amounts of underlying data and thus to provide even more confidence in the ARES tool results.

The MASTER model is currently being upgraded. Additional measurement campaigns and an update of the event database have been performed and are currently used in the validation process. Moreover, a new feature of MASTER will be uncertainties provided along with the nominal flux values. The idea is to derive uncertainties from the model deviations obtained during the validation process. This requires an even more careful consideration of all the intricacies of the involved sensors and retrieved surfaces, as well as a weighting scheme reflecting the quantity but also the quality of the collected data.

For future MASTER versions, additional sources of information will be investigated to be implemented in the validation process, like in-situ detectors or alternative catalogues like the bulletin provided by the JSC Vimpel Interstate Corporation and the Keldysh Institute of Applied Mathematics. This requires additional automation in the iterative validation process in order to obtain an optimal representation of the space debris and micrometeoroid population by the model, especially in view of the model being increasingly used in the requirement verification process of satellite missions.

REFERENCES

1. Braun, V. (2016). Operational support to collision avoidance activities by ESA's space debris office. *CEAS Space Journal* **8**.3, 177–189. DOI: 10.1007/s12567-016-0119-3.
2. Bunte, K. D., Destefanis, R, and Drolshagen, G (2009). Spacecraft Shielding Layout and Optimisation Using ESABASE2/Debris. 5^{th} *European Conference on Space Debris, Darmstadt*.
3. *European Code of Conduct for Space Debris Mitigation* (2004). Issue 1.0.
4. European Cooperation for Space Standardization (ECSS) (2008). *Space engineering - Space environment*. ECSS-E-ST-10-04C.
5. — (2012). *Adoption Notice of ISO 24113: Space systems - Space debris mitigation requirements*. ECSS-U-AS-10C.
6. Flegel, S. K. (2013). *Multi-layer Insulation as Contribution to Orbital Debris*. Dissertation, Technische Universität Braunschweig.
7. Flegel, S., Gelhaus, J., and Möckel, M. (2011). Maintenance of the ESA MASTER model. *Final Report, ESA contract 21705/08/D/HK*.
8. Foster, J. L. (1992). *A parametric analysis of orbital debris collision probability and maneuver rate for space vehicles*. NASA JSC-25898.
9. *French Space Operations Act* (2008). 2008-518.
10. Gelhaus, J. (2014). Upgrade of ESA's Space Debris Mitigation Analysis Tool Suite. *Final Report, ESA contract 4000104977/11/D/SR*.
11. International Organization for Standardization (ISO) (2011). *Space systems - Space debris mitigation requirements*. ISO 24113:2011.
12. Johnson, N. (2001). NASA's new breakup model of EVOLVE 4.0. *Advances in Space Research* **28**.9, 1377 –1384.
13. Klinkrad, H. (2002). Monitoring Space–Efforts Made by European Countries. *International Colloquium on Europe and Space Debris, sponsored by the Académie National de lAir et de lEspace, Toulouse, France*.
14. Klinkrad, H. (1997). An Introduction to the 1997 ESA MASTER Model. *Second European Conference on Space Debris, Darmstadt*.

15. Krisko, P. (October 2011). Proper Implementation of the 1998 NASA Breakup Model. *Orbital Debris Quarterly News* **15**.4.
16. Krisko, P. and Foster, J. (2007). Modeling the sodium potassium droplet interactions with the low earth orbit space debris environment. *Acta Astronautica* **60**.10, 939–945.
17. Markkanen, J., Lehtinen, M., and Landgraf, M (2005). Real-time space debris monitoring with EISCAT. *Advances in Space Research* **35**.7, 1197–1209.
18. Martin, C. (2005). Debris Risk Assessment and Mitigation Analysis (DRAMA) Tool. *Final Report, ESA contract 16966/02/D/HK*.
19. Schildknecht, T (2001). Optical observation of space debris in the geostationary ring. *Space Debris*. Vol. 473, pp. 89–93.
20. Stabroth, S. (2007). Explanation of the "May Swarm" signature in the LDEF IDE impact data. *Aerospace Science and Technology* **11**.2-3, 253–257.
21. Stabroth, S. (2008). Identification of Solid Rocket Motor Retro-Burns in the LDEF IDE Impact Data. *AIAA/AAS Astrodynamics Specialist Conference, Honolulu, HI*.
22. The Consultative Committee for Space Data Systems (CCSDS) (2013). *Conjunction Data Message, Recommended Standard*. CCSDS 508.0-B-1, Blue Book.
23. Wiedemann, C. (2009). Additional historical solid rocket motor burns. *Acta Astronautica* **64**.11, 1276 –1285. DOI: http://dx.doi.org/10.1016/j.actaastro.2009.01.011.
24. Wiedemann, C. (2016). Release of liquid metal droplets from Cosmos 1818 and 1867. *IAC-16.A6.2.9,* 67^{th} *International Astronautical Congress (IAC), Guadalajara*.
25. — (2017). The Contribution of NaK Droplets to the Space Debris Environment. *Seventh European Conference on Space Debris, Darmstadt*.